Vehicle System Dynamics: International Journal of Vehicle Mechanics and Mobility

Publication details, including instructions for authors and subscription information:
http://www.tandfonline.com/loi/nvsd20

Parameter and state estimation for articulated heavy vehicles

Caizhen Cheng [a] & David Cebon [a]

[a] Engineering Department, Cambridge University, Trumpington Street, Cambridge, CB2 1PZ, UK

Published online: 15 Jul 2010.

To cite this article: Caizhen Cheng & David Cebon (2011): Parameter and state estimation for articulated heavy vehicles, Vehicle System Dynamics: International Journal of Vehicle Mechanics and Mobility, 49:1-2, 399-418

To link to this article: http://dx.doi.org/10.1080/00423110903406656

Vehicle System Dynamics
Vol. 49, Nos. 1–2, January–February 2011, 399–418

Taylor & Francis
Taylor & Francis Group

Parameter and state estimation for articulated heavy vehicles

Caizhen Cheng and David Cebon*

Engineering Department, Cambridge University, Trumpington Street, Cambridge CB2 1PZ, UK

(*Received 24 March 2009; final version received 5 October 2009; first published 15 July 2010*)

This article discusses algorithms to estimate parameters and states of articulated heavy vehicles. First, 3- and 5-degrees-of-freedom linear vehicle models of a tractor semitrailer are presented. Vehicle parameter estimation methods based on the dual extended Kalman filter and state estimation based on the Kalman filter are presented. A program of experimental tests on an instrumental heavy goods vehicle is described. Simulation and experimental results showed that the algorithms generate accurate estimates of vehicle parameters and states under most circumstances.

Keywords: parameter estimation; state estimation; Kalman filter; dual extended Kalman filter; articulated vehicle

1. Introduction

Some control strategies require the feedback of vehicle states which cannot be measured easily. Among all vehicle states, sideslip is a very important variable for vehicle dynamics and control [1–3]. The accuracy of the sideslip measurement has a significant effect on vehicle control. The sideslip angle can be measured using either optical or Global Positioning System (GPS) sensors. However, these methods have practical issues of cost, accuracy, and reliability, that limit their use in production vehicles [4].

Many approaches have been proposed to estimate the sideslip angle, or equivalently the lateral velocity, in the literature. Among them, the most commonly used method is a model-based estimator with Kalman filter (KF). In 1960, Kalman [5] published his paper describing a recursive solution to the discrete-time linear filtering problem. Since then, the KF has been the subject of extensive research and application.

Zuurbier *et al.* [6] developed a vehicle controller and a state estimator for a combined braking and chassis control system to improve the handling of an automobile. The state estimator was based on a nonlinear vehicle model combined with an extended Kalman filter (EKF), which was connected to another estimation algorithm for the tyre-road friction coefficient.

*Corresponding author. Email: dc@eng.cam.ac.uk

ISSN 0042-3114 print/ISSN 1744-5159 online

DOI: 10.1080/00423110903406656
http://www.informaworld.com

There are some reports on other estimation methods for estimating sideslip. Hac and Simpson [7] presented an algorithm for estimating vehicle yaw rate and sideslip angle using steering wheel angle, wheel speed, and lateral acceleration sensors. The algorithm was tested on various surfaces for handling manoeuvres. The results showed that the algorithm gave good etimates of yaw rate and sideslip, even in extreme manoeuvres.

In 2004, Ungoren and Peng [8] presented a study on three approaches to vehicle lateral speed estimation: transfer function approach, state–space approach, and kinematics approach. The first two methods rely on a vehicle dynamics model, and the last approach is based on the kinematic relationships of the measured signals. The performance of these three methods was investigated using simulation and experimental data. The authors concluded that each method would need to be improved before it could be used alone, or an integrated system could be developed to produce reliable lateral speed estimation.

In order to estimate the vehicle states and design an active controller using a model-based estimation approach, an accurate set of parameters is needed for the vehicle model. This means that some vehicle parameters (e.g. tyre cornering stiffness) must first be estimated. Sienel [9] reported a method for estimating the tyre cornering stiffness of the front axle of a car, based on the measurements of front steering angle, yaw rate, and lateral acceleration at the front axle. Simulation results showed that the estimates of the tyre cornering stiffness to match well with the values in the vehicle model.

In 2006, Kober and Hirschberg [10] presented a paper concerned with on-board payload identification for commercial vehicles. The identification system was based on the measured pressures of the vehicle's air springs and its lateral acceleration. The identified parameters include the load mass, the position of its centre of gravity and especially the height of its centre of gravity. The identified results can be used as driver information or delivered to vehicle dynamics controllers.

In 2006, Wenzel *et al.* [11] reported implementation of the dual extended Kalman filter (DEKF) technique for vehicle state and parameter estimation using two interdependent KFs running in parallel. The parameter estimator can be switched off, once a sufficiently good set of parameter estimates has been achieved. The potential benefits of DEKF were shown using both simulation and vehicle test data. But it was also concluded that appropriate selection of the process noise covariance matrix is a key factor for the parameter estimation.

Extensive research has been done on parameter and state estimation of passenger cars. However, papers on parameter and state estimation for articulated heavy vehicles are few. Little has been found on the key issues of the estimation of tyre cornering stiffness and trailer's Centre of Gravity (CoG) position of articulated heavy vehicles.

This article, therefore, deals with parameter and state estimation methods for articulated heavy vehicles. The modelling is presented in Section 2, including linear vehicle models, parameter estimation algorithm with DEKF, and state estimation algorithm with KF. Simulation and experimental results are presented in Sections 3 and 4, respectively.

2. Modelling

2.1. *Linear vehicle models*

Two different vehicle models are used in the estimation process. A 3-degrees-of-freeedom (DOF) sideslip/yaw model is used for estimating some of the parameters and a 5-DoF linear sideslip/roll/yaw vehicle model is used for estimating the remaining parameters and vehicle states. These models embody the most important aspects of articulated vehicle handling. The coordinate system of tractor semitrailer is shown in Figure 1.

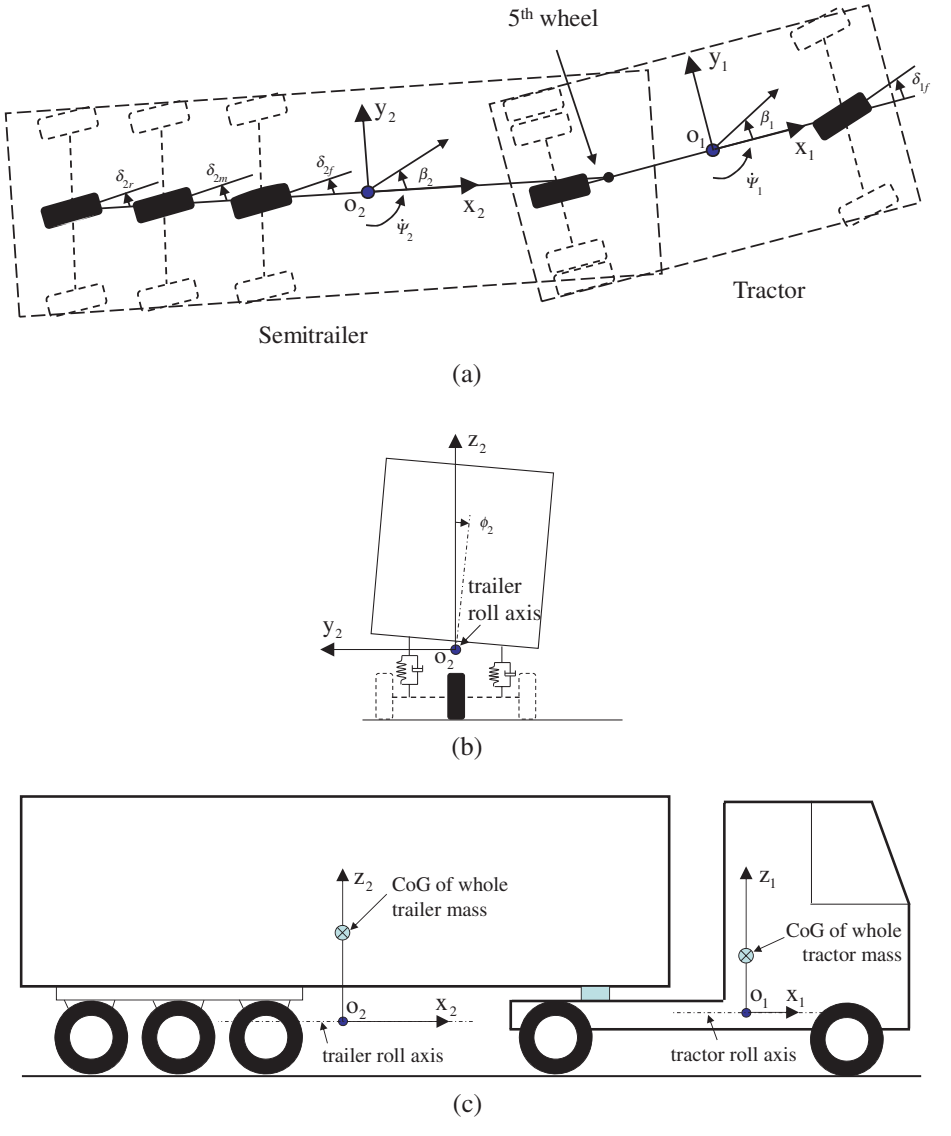

Figure 1. Vehicle-fixed coordinate system of tractor semitrailer with the possibility of trailer wheel steering (a) top view of tractor semitrailer; (b) rear view of semitrailer; (c) side view of tractor semitrailer.

2.1.1. *5-DoF linear sideslip/roll/yaw vehicle model*

The 5-DoF sideslip/roll/yaw linear vehicle model has two rigid bodies: the tractor and the semitrailer. The DOFs are tractor sideslip, tractor yaw and roll, and semitrailer yaw and roll.

The assumptions for the linear vehicle model are as follows:

- The forward speed is a slow-changing state.
- Vehicle parameters are constant but vary with payload.
- The tractor and semitrailer units have no pitch or bounce.
- The angular displacements during the manoeuvres are small, the articulation angle between the tractor and the semitrailer units is small, and the vehicle dynamics are considered as linear.

- The roll stiffness and damping of the vehicle suspension systems are constant in the range of roll motions involved.
- Both wheels on an axle have the same slip angle and are modelled as a single wheel as per the 'bicycle' model approach.
- The cornering stiffnesses of the three trailer axles are the same.
- The effects of side wind and road slope are neglected.

The equations representing the 5-DoF linear vehicle are given in the Appendix. Detailed derivative of the equations can also be found in [12–14]. The state–space representation of these equations is given by

$$\dot{\mathbf{x}} = \mathbf{A}\mathbf{x} + \mathbf{B}\mathbf{u}, \tag{1}$$

where $\mathbf{x} = \begin{bmatrix}\phi_1 & \dot{\phi}_1 & \beta_1 & \dot{\psi}_1 & \phi_2 & \dot{\phi}_2 & \beta_2 & \dot{\psi}_2\end{bmatrix}^{\mathrm{T}}$ and $\mathbf{u} = \begin{bmatrix}\delta_{1f} & \delta_{2f} & \delta_{2m} & \delta_{2r}\end{bmatrix}^{\mathrm{T}}$.

The discrete-time formulation of state–space representation is given by

$$\mathbf{x}_{k+1} = \mathbf{A}_d\mathbf{x}_k + \mathbf{B}_d\mathbf{u}_k. \tag{2}$$

The subscript k denotes the discrete-time instant kT, and T is the time step.

2.1.2. *3-DoF linear yaw vehicle model*

A 3-DoF linear yaw vehicle model was used to design the parameter estimation algorithm for tyre cornering stiffnesses and trailer yaw moment of inertia. This model is a simplified version of the 5-DoF linear vehicle model described previously. The tractor is free to sideslip and yaw, and the semitrailer can yaw relative to the trailer, but the equations and variables related to roll motion. The equations of the 3-DoF vehicle model can also be expressed using the state–space representations in Equations (1) and (2), with $\mathbf{x} = \begin{bmatrix}\beta_1 & \dot{\psi}_1 & \beta_2 & \dot{\psi}_2\end{bmatrix}^{\mathrm{T}}$.

2.2. *Theory*

2.2.1. *Introduction*

In this article, a model-based estimator with the 5-DoF linear vehicle model is proposed to estimate the vehicle states. In order to implement the estimator, all the vehicle parameters in the 5-DoF linear vehicle model need to be known.

Some of the vehicle parameters do not change with different payloads, such as tractor yaw and roll moments of inertia and height of the tractor sprung mass CoG. These parameters are assumed to be known. They could be obtained from the tractor manufacturer or calculation, or by measurements.

A second group of vehicle parameters may vary with payloads, but they can be available from the manufacturer, or by rough estimation as well. These include suspension roll stiffness and damping ratio, the axle roll stiffness caused by tyre deflection, and the roll stiffness of the hitch point (fifth wheel) between tractor and semitrailer.

Among the rest of the vehicle parameters required by the model, some can be calculated based on the static axle loads, as could be measured by an on-board axle weighing system (e.g. using air spring pressure sensor). These include the masses of tractor and semitrailer, and the longitudinal CoG positions of tractor and semitrailer. These values are regarded as constant if the payload condition is not changed. The weights and CoG positions used in the simulations reported here were based on measured axle weights.

Apart from the above parameters, there are still some key vehicle parameters that remain unknown. These are the tyre cornering stiffnesses, trailer roll and yaw moments of inertia, and the height of trailer sprung mass CoG. In order to estimate these vehicle parameters, estimation algorithms based on the DEKF technique are introduced below.

Initial simulation results showed that the accuracies of parameter estimation were not good, and the estimation values did not converge in some circumstances, when all the vehicle parameters (tyre cornering stiffnesses, trailer roll and yaw moments of inertia, height of trailer sprung mass CoG) were estimated at the same time using the DEKF. Consequently, a two-step procedure was developed to estimate all vehicle parameters.

Figure 2 shows the overall estimation process. In 'parameter estimation stage 1', the tyre cornering stiffnesses and the trailer yaw moment of inertia are estimated using the 3-DoF linear yaw vehicle model. These parameters are then assumed fixed in 'parameter estimation stage 2', when the height of trailer sprung mass CoG and the trailer roll moment of inertia about the trailer roll axis is estimated with the 5-DoF linear vehicle model.

When all the vehicle parameters are known, the vehicle states are estimated by a model-based estimator with KF.

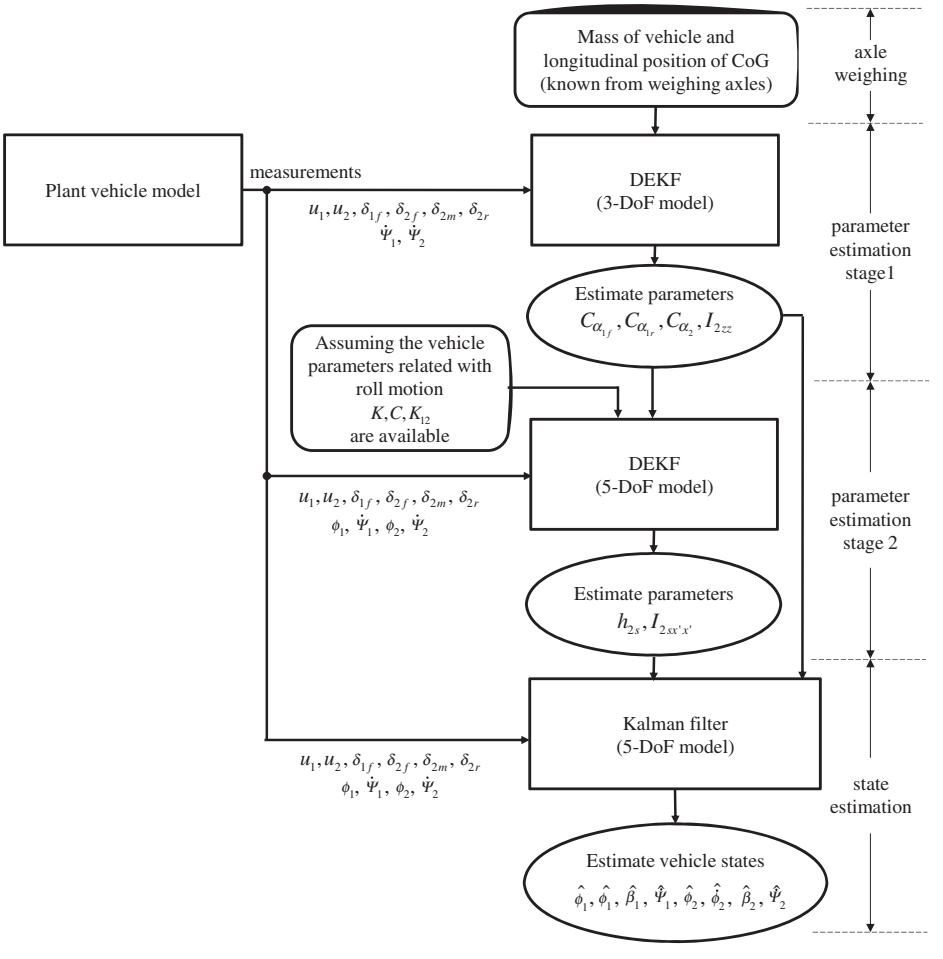

Figure 2. Parameter and state estimation process.

2.2.2. *Kalman filter*

The KF is an efficient recursive filter that can estimate the states of a dynamic system from a series of incomplete and noisy measurements.

The linear vehicle model can be formulated as follows:

$$\mathbf{x}_{k+1} = \mathbf{A}_d \mathbf{x}_k + \mathbf{B}_d \mathbf{u}_k + \mathbf{w}_k, \tag{3}$$

$$\mathbf{y}_k = \mathbf{C}_d \mathbf{x}_k + \mathbf{D}_d \mathbf{u}_k + \mathbf{v}_k, \tag{4}$$

where $\mathbf{x}$ is the state vector, $\mathbf{u}$ the input vector, $\mathbf{y}$ the output vector, with $\mathbf{w}$ and $\mathbf{v}$ being the process and output noise vectors, respectively. $\mathbf{w}$ and $\mathbf{v}$ are assumed to be independent white Gaussian noise process.

$$p(\mathbf{w}) \sim N(0, \mathbf{Q}), \tag{5}$$

$$p(\mathbf{v}) \sim N(0, \mathbf{R}), \tag{6}$$

where N(,) means a normal probability distribution.

The process noise covariance matrix $\mathbf{Q}$ and the measurement noise covariance matrix $\mathbf{R}$ could vary at each time step. However, they are assumed to be constant in this article. The measurement noise covariance matrix $\mathbf{R}$ can be determined from the measured signals on the experimental vehicle.

2.2.3. *Dual extended Kalman filter*

Wan and Nelson [15,16] presented reviews of the EKF for both state and parameter estimation. They introduced the DEKF, which is a combined state and parameter estimation algorithm using two EKFs in parallel.

Figure 3 schematically illustrates the operation scheme of the DEKF. At each time step, the 'state EKF' generates state estimates, and requires a vector of parameters $\hat{\mathbf{p}}_{k-1}$ for the time update. The 'parameter EKF' generates parameter estimates, and requires a vector of states $\hat{\mathbf{x}}_{k-1}$ for the measurement update. The detailed equations of the DEKF are given in [17].

For finite data sets, the algorithm can run iteratively over the data until the parameters converge [18]. In addition, the parameter covariance matrix $\mathbf{Q}_p$ can be adjusted by repeatedly

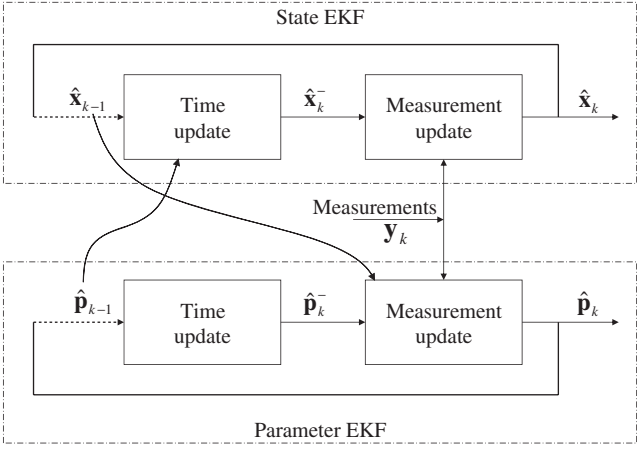

Figure 3. Operation scheme of the DEKF.

multiplying by a 'forgetting factor' $\lambda(0 < \lambda < 1)$ at each time step. This will enhance the convergence of the parameter estimation in the DEKF for a linear vehicle system. Simulation results, in the following, show that the parameters in the DEKF can effectively converge to the reference values. Refer to Cheng [17] for further details.

Both EKFs are needed to estimate the parameters; however, for state estimation, it is possible to switch off the parameter estimator, once a sufficiently good set of parameter estimates has been achieved. In this article, the parameter estimates are determined by averaging the estimated values for the rest of the estimation process, after their estimation variations are reduced within a small amount of percent (e.g. ±1%). This leaves the state estimator function only. This should increase the accuracy of the state estimator, because it reduces the parameter uncertainties.

2.2.4. *Parameter estimation stage 1 (C_a, I_{2zz})*

The tyre cornering stiffnesses C_a and the trailer yaw moment of inertia I_{2zz} are estimated by DEKF with the 3-DoF linear yaw vehicle model based on the knowledge of the mass of each vehicle unit and the longitudinal position of its CoG. The tractor yaw moment of inertia is assumed to be available as well. The tyres are assumed to be linear (i.e. the cornering stiffnesses of each axle are assumed to be constant) with varying slip angle and lateral load transfer. This is reasonable for small steer angles. To simplify the estimation process, the tyre cornering stiffnesses of all tyres on the trailer are lumped together into a single value as follows:

$$C_{\alpha_2} = C_{\alpha_{2f}} + C_{\alpha_{2m}} + C_{\alpha_{2r}}, \tag{7}$$

where $C_{\alpha_{2f}}$, $C_{\alpha_{2m}}$, and $C_{\alpha_{2r}}$ are the cornering stiffness of front/middle/rear trailer axles (N/rad)

The measured signals include the longitudinal vehicle speed, front wheel steering angle, trailer wheel steering angles, yaw rate of tractor, and yaw rate of semitrailer. The estimated vehicle parameters include tyre cornering stiffnesses of tractor steering axle, tractor drive axle and trailer axles, and the trailer yaw moment of inertia.

2.2.5. *Parameter estimation stage 2 (h_{2s}, $I_{2sx'x'}$)*

Based on known axle weights and parameters from estimation stage 1 (see Figure 2), the height of trailer sprung mass CoG, h_{2s}, and the trailer roll moment of inertia about the trailer roll axis, $I_{2sx'x'}$, are estimated by DEKF with the 5-DoF linear vehicle model.

Because the height of the trailer sprung mass CoG and the trailer roll moment of inertia are interdependent, initial simulations showed that, when estimated simultaneously, the estimated values of these two parameters would not converge.

The approach taken was, therefore, to assume a uniformly distributed payload; to estimate the payload height by DEKF and hence to calculate the height of trailer sprung mass CoG and the trailer roll moment of inertia.

The following assumptions were necessary to perform the calculation:

- The height of unladen trailer sprung mass CoG is known.
- The unladen trailer roll moment of inertia around the roll centre of trailer is known.
- The payload is uniformly distributed across the area of the trailer box.
- The height of the trailer floor is known from the measurement.
- The vertical distance between the trailer roll centre and the trailer floor does not change with payload.

With the estimated height of payload from the trailer floor, h_{2p}, the height of trailer sprung mass CoG and trailer roll moment of inertia around the trailer roll centre can be calculated as follows:

$$h_{2s} = \frac{h_{2s_e} m_{2s_e} + (h_{2f} + (h_{2p}/2))(m_{2s} - m_{2s_e})}{m_{2s}}, \tag{8}$$

$$I_{2sx'x'} = I_{2sx'x'_e} + \frac{1}{12}(m_{2s} - m_{2s_e})((D_p)^2 + (h_{2p})^2) + (m_{2s} - m_{2s_e})\left(h_{2f} + \frac{h_{2p}}{2} - h_{2r}\right)^2, \tag{9}$$

where h_{2s_e} is the height of empty trailer sprung mass CoG (m), m_{2s_e} the empty trailer sprung mass (kg), h_{2f} the height of trailer floor from the ground (m), h_{2p} the height of payload from the trailer floor (m), h_{2r} height of trailer roll axis from the ground (m), $I_{2sx'x'_e}$ the roll moment of inertia of empty trailer sprung mass around trailer roll axis (kgm^2), and D_p the width of payload in trailer (m).

The measured signals include the longitudinal vehicle speed, front wheel steering angle, trailer wheel steering angles, tractor roll rate and yaw rate, and trailer roll rate and yaw rate.

2.3. *Vehicle state estimation*

Using the approach described above, all the vehicle parameters, including the mass, moment of inertia, dimensional parameters, tyre cornering stiffnesses, etc., can be found step-by-step.

Vehicle states can then be estimated using a KF with a limited number of noisy measurements. The measured signals can be divided into two groups. One group is system inputs, including longitudinal vehicle speed, tractor front wheel steering angle, and trailer axle steering angles. The other group is system outputs, including roll rate and yaw rate of tractor, and roll rate and yaw rate of semitrailer.

The unmeasured vehicle states, estimated by the KF, are roll angle and sideslip of the tractor, and roll angle and sideslip of the semitrailer.

3. Simulation

3.1. *Introduction*

Simulation results are described in this section to verify the estimation algorithms. Only the condition with fully laden trailer is discussed in this article. Other test cases are detailed in [17].

A standard high-speed SAE J2179 lane change [19] was used to determine vehicle parameters and state estimation. The vehicle followed a half-sinusoidal 'lane change' path with an offset of 1.464 m, in the distance of 61 m, at a speed of 88 km/h. Repetitions of this lane change were used for the parameter estimation.

The offset magnitude of the lane change manoeuvre for parameter estimation depends on the signal-to-noise ratio. Generally, the more severe the lane change (with the vehicle tyres still in, or near, their linear region), the more accurate the estimated parameters should be. For state estimation, any driving manoeuvre is acceptable, even a straight line manoeuvre with a constant vehicle speed.

For parameter estimation, the process noise covariance matrix $\mathbf{Q}_x$ was set to zero. While for the vehicle state estimation, the process noise covariance matrix $\mathbf{Q}_x$ was set to a small diagonal matrix, that is, $\mathbf{Q}_x = \mathbf{I} \times 10^{-8}$, where $\mathbf{I}$ is an identity matrix.

In addition, a forgetting factor λ was used in the DEKF algorithm [16], working together with the parameter covariance matrix $\mathbf{Q}_p$. The parameter covariance matrix $\mathbf{Q}_p$ was repeatedly multiplied by the forgetting factor λ at each time step. The forgetting factor λ allows the DEKF to apply less emphasis on previous information about parameter uncertainties as time grows.

The initial values of the estimated vehicle parameters were set as either 80% or 120% of the values in the plant vehicle model.

Simulations using the same vehicle models for the plant, and in the estimation algorithms, proved the correctness of the estimation algorithms and the feasibility of using repetitions of a lane change as the driving manoeuvre for parameter estimation. The simulation results presented here are for the much more realistic nonlinear plant vehicle model in TruckSim [17]. This model includes translational and rotational motions of tractor and semitrailer, vertical and roll motions of each axle, wheel steer, and wheel rotation. The most important source of nonlinearity in the model is the side force behaviour of the tyres, which is a nonlinear function of slip angle and normal load.

The measurements used in the KF are outputs from the TruckSim model with added white Gaussian noise.

The parameter estimation results for tyre cornering stiffnesses and trailer yaw moment of inertia are given in Section 3.2. Then, the parameter estimation results of the height of payload are given in Section 3.3. Finally, the state estimation results are given in Section 3.4.

3.2. *Tyre cornering stiffnesses and trailer yaw moment of inertia*

The DEKF with the 3-DoF vehicle model was used to estimate the tyre cornering stiffnesses and trailer yaw moment of inertia. The simulated measurements were tractor yaw rate $\dot{\psi}_1$ and trailer yaw rate $\dot{\psi}_2$. The corresponding measurement noise covariance matrix $\mathbf{R}$ was determined from measured sensor noise levels on the test vehicle as follows:

$$\mathbf{R} = \begin{bmatrix} 1.52 \times 10^{-5} & 0 \\ 0 & 1.11 \times 10^{-5} \end{bmatrix} \begin{bmatrix} \dot{\psi}_1 \\ \dot{\psi}_2 \end{bmatrix}. \tag{10}$$

(The diagonal elements of $\mathbf{R}$ have dimensions of [noise units]^2, in this case (rad/s)^2.)

The initial parameter covariance matrix $\mathbf{Q}_p$ was set as follows:

$$\mathbf{Q}_p = \begin{bmatrix} (475)^2 & 0 & 0 & 0 \\ 0 & (766)^2 & 0 & 0 \\ 0 & 0 & (1273)^2 & 0 \\ 0 & 0 & 0 & (413)^2 \end{bmatrix} \begin{bmatrix} C_{\alpha_{1f}} \\ C_{\alpha_{1r}} \\ C_{\alpha_2} \\ I_{2zz} \end{bmatrix}, \tag{11}$$

where the square root of the terms of $\mathbf{Q}_p$ (475, etc.) is 0.1% of the nominal values of the estimated parameters. The forgetting factor λ was set as 0.999.

Figure 4 shows the estimation results for the tyre cornering stiffnesses of the trailer axles and trailer yaw moment of inertia. The estimated values are shown as dashed lines, while the reference value is a solid line in Figure 4b. Since the values of tyre cornering stiffnesses in TruckSim vary with slip angle and vertical load, the approximate range of the reference values is shown as dash–dot lines in Figure 4a. These were determined by running the vehicle simulation in TruckSim at 88 km/h, with front wheel steering angle at 0.1° and 1°. With 1° front wheel steering, the tyre sideslip angles of each axle are close to the maximum values of tyre sideslip angles in the lane change.

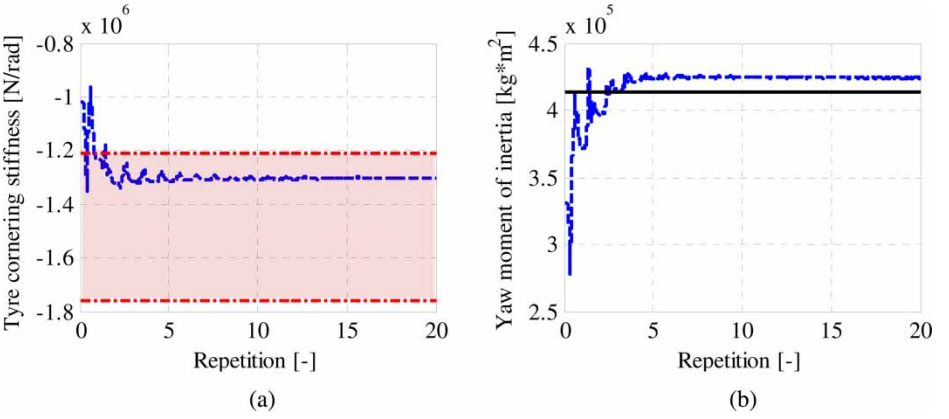

Figure 4. Estimation of C_α and I_{2zz} in TruckSim: (a) tyre cornering stiffness of all tyres on trailer axles and (b) trailer yaw moment of inertia. Estimated values (– – –), range of reference values (– · – · –), reference values (———).

The estimated values of linearised tyre cornering stiffnesses and trailer yaw moment of inertia are $C_{\alpha_{1f}} = -4.77 \times 10^5$ N/rad, $C_{\alpha_{1r}} = -8.98 \times 10^5$ N/rad, $C_{\alpha_2} = -1.30 \times 10^6$ N/rad, and $I_{2zz} = 4.24 \times 10^5$ kgm^2. The estimation error for the trailer yaw moment of inertia is 2.5%, relative to the reference value in TruckSim model. It is due to the nonlinearity in the TruckSim model.

3.3. *Height of trailer sprung mass CoG and trailer roll moment of inertia*

The height of the payload from the trailer floor was estimated using the DEKF with the 5-DoF model.

The simulated measurements were tractor roll rate $\dot{\phi}_1$, trailer roll rate $\dot{\phi}_2$, tractor yaw rate $\dot{\psi}_1$, and trailer yaw rate $\dot{\psi}_2$. The corresponding measurement noise covariance matrix $\mathbf{R}$ was set as follows:

$$\mathbf{R} = \begin{bmatrix} 4.52 \times 10^{-4} & 0 & 0 & 0 \\ 0 & 4.70 \times 10^{-5} & 0 & 0 \\ 0 & 0 & 1.52 \times 10^{-5} & 0 \\ 0 & 0 & 0 & 1.11 \times 10^{-5} \end{bmatrix} \begin{bmatrix} \dot{\phi}_1 \\ \dot{\phi}_2 \\ \dot{\psi}_1 \\ \dot{\psi}_2 \end{bmatrix}. \quad (12)$$

The initial parameter covariance matrix $\mathbf{Q}_p$ was set as follows:

$$\mathbf{Q}_p = [(0.005)^2] h_{2p}, \quad (13)$$

where 0.005 is approximately 0.5% of the nominal values of the estimated height of the payload. The forgetting factor λ was set as 0.999. The initial value of the height of payload was set as 0.1 m, which is much less than the actual value 1.23 m. The estimated results of tyre cornering stiffnesses and trailer yaw moment of inertia from parameter estimation stage 1 (Section 3.2) were used in the estimation stage 2.

Figure 5 shows the estimated payload height. The estimated value is 1.237 m, shown as dashed line. The reference value from the TruckSim model is 1.23 m, shown as solid line. It can be seen that the estimated value of the height of payload is very close to the reference value. The estimation error is about 0.6%.

Based on the estimated payload height, the height of trailer sprung mass CoG and the trailer roll moment of inertia around the trailer roll axis were calculated using Equations (8) and (9)

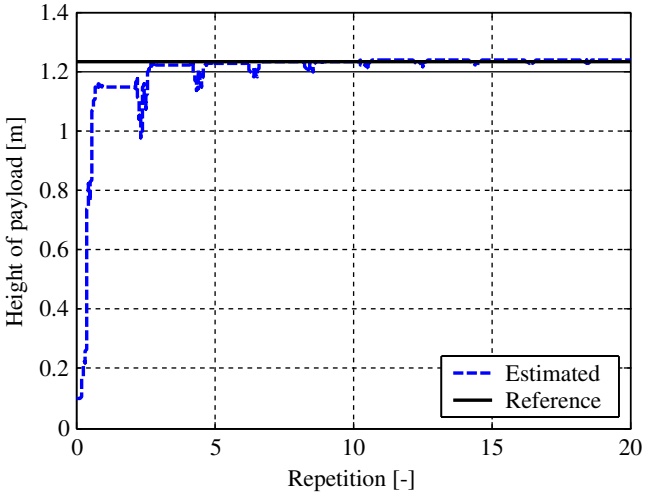

Figure 5. Estimation of h_{2p} in TruckSim.

as $h_{2s} = 1.602$ m and $I_{2sx'x'} = 4.35 \times 10^4$ kgm^2. These values are accurate within 0.1% and 0.4%, respectively.

The simulation of parameter estimation with non-uniform payload distribution in TruckSim was also examined. Instead of assuming that the trailer payload is uniformly distributed across the rectangular area of the trailer box, it was assumed that it occupies a point along the trailer centre line with the effective height of payload.

The estimated value of the height of payload in this case was 1.084 m. The estimation error is about 11.9%, relative to the reference value of 1.23 m in the TruckSim model.

Based on the estimated payload height, the height of trailer sprung mass CoG and the trailer roll moment of inertia around the trailer roll axis [see Equations (8) and (9)] were calculated as $h_{2s} = 1.553$ m and $I_{2x'x'} = 3.99 \times 10^4$ kgm^2. The estimation errors are 2.9% and 20%, respectively, relative to the reference values of 1.6 m and 33,308 kgm^2. The estimation error is caused by that the estimation algorithm assuming the payload is uniformly distributed while it is actually not in the TruckSim plant model. In the extreme condition, the algorithms still gave good estimates of the height of trailer sprung mass CoG and the trailer roll moment of inertia. Refer to Cheng [17] for details.

3.4. *Vehicle state estimation*

Once all vehicle parameters were available from the parameter estimation, the performance of the state estimation was examined in simulation with the TruckSim vehicle model.

The simulated measurements were tractor roll rate $\dot{\phi}_1$, trailer roll rate $\dot{\phi}_2$, tractor yaw rate $\dot{\psi}_1$, and trailer yaw rate $\dot{\psi}_2$. The corresponding measurement noise covariance matrix $\mathbf{R}$ is set the same as in Equation (12). While the process noise covariance $\mathbf{Q}_x$ is set as follows:

$$\mathbf{Q}_x = \mathbf{I} \times 10^{-8}, \tag{14}$$

where $\mathbf{I}$ is an 8×8 identify matrix.

Figure 6 shows the estimated trailer states in the lane change manoeuvre. It can be seen from Figure 6c that the estimated trailer's sideslip is very close to the reference value from the vehicle model in TruckSim. The largest differences between the estimated and the reference

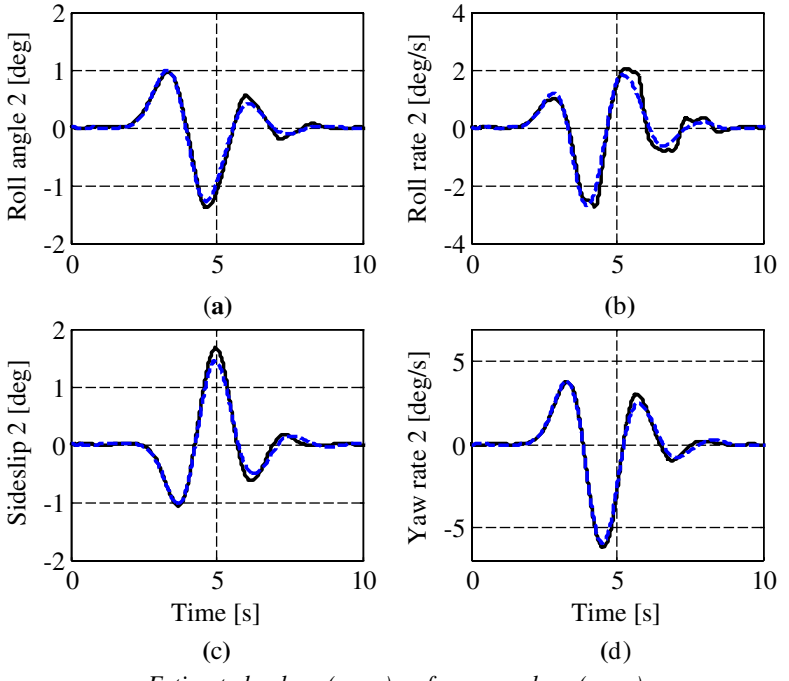

Figure 6. Estimated states of the TruckSim model in lane change manoeuvre: (a) roll angle of sprung mass of trailer; (b) roll rate of sprung mass of trailer; (c) sideslip angle of sprung mass of trailer; and (d) yaw rate of sprung mass of trailer.

values occur at sections with high sideslip values. These differences are due to the reduction of effective tyre cornering stiffnesses in TruckSim with lateral load transfer and tyre slip. These nonlinear effects were ignored in the estimation algorithms.

4. Experiment

4.1. *Introduction*

To investigate the viability and practicality of the estimation approach, an instrumented test vehicle, comprising a two-axle tractor unit and a three-axle semitrailer unit, was used. The vehicle parameter and state estimation algorithms were verified through a series of tests.

4.1.1. *Vehicle configuration*

The vehicle used in the testing was the Cambridge Vehicle Dynamics Consortiums (CVDC) experimental vehicle with active steering trailer. The CVDC tractor is a Volvo FH-12 4 × 2, which has been fitted with a variety of sensors. It is typical of two-axle tractors used throughout UK and the European Union. Further details about the tractor unit can be found in [20,21].

The active steering trailer is a 12.5 m long tri-axle trailer fitted with active steering axles developed by CVDC. All axles on the trailer were locked during the experiment, for this study of parameter and state estimation. Further details of the steering system are given in [22].

The floor of the trailer was fitted with 18 ballast water tanks, which were uniformly distributed. The trailer with fully filled water tanks is near full UK legal weight limits for this vehicle configuration: 38 tonne Gross Vehicle Weight (GVW). The trailer was also fitted with outriggers on each side to prevent rollover during extreme manoeuvres.

4.1.2. *Signal logging system*

A distributed, multi-level control system was used to log the signal data from all sensors, and the trailer's steering system. It was based on the distributed control system which was first developed for the CVDC's roll/ride vehicle [20,21], and then adapted for the steering trailer project in [22].

Signals from the sensors on the tractor and semitrailer units were passed to two 'ICON' industrial computers, one on each vehicle unit. These signals were filtered, digitised, and processed in the local controllers before being transmitted to a central 'Global Control Computer' in the tractor unit, via the vehicle's CANbus communication network. The global controller stored the data for each test and a laptop computer was used to retrieve the data from the global controller and save it for post-processing. Further details of this logging system can be found in [20,21]. The ICON computer on the steering trailer was specifically built and commissioned for the steering projects. Further details can be found in [22].

4.1.3. *Sensors*

The CVDC experimental vehicle is fitted with a number of sensors to measure key vehicle states. The measured tractor's states in this project include the front wheel steering angle, longitudinal vehicle speed, roll rate, and yaw rate. Further details about these sensors are given in [20,21,23].

The CVDC steering trailer unit is also fitted with a number of sensors. The sensor signals used in this project include the roll rate, yaw rate, and the steering actuator displacement on each axle (used to determine the steering angle of each trailer axle). See Jujnovich and Cebon [22] for further details.

In order to determine the accuracy of the estimated sideslip of trailer, a Corrsys–Datron two-axis optical sensor was fitted to the trailer to measure the sideslip. It was mounted on a cross beam at the position of landing leg of the trailer. The distance between the optical sensor and the fifth wheel was 2.34 m, and the wheel base of trailer was 8.0 m. This optical sensor takes a series of images of the road surface and uses correlation between images to determine the longitudinal vehicle speed and sideslip angle. Refer to [24] for more details about the optical sensor.

4.1.4. *Test manoeuvres*

Vehicle testing was conducted at the Motor Industry Research Association (MIRA) proving ground at Nuneaton, Warwickshire, UK, in November 2006. The vehicle was subjected to a lane change manoeuvre, to validate the parameter and state estimation algorithms.

The length of the lane change was 30 m and its lateral offset was 4 m. The testing track is dry 'delugrip' surface, whose nominal coefficient of friction is 0.75. The nominal path for the manoeuvre was marked on the test track with yellow tape. The vehicle speed was kept constant for each test. Three runs were performed to ensure repeatability. See Cheng [17] for further details of these tests.

4.2. *Tyre cornering stiffnesses and trailer yaw moment of inertia*

Some initial investigation showed that the estimation results were not accurate, if all tyre cornering stiffnesses $C_{\alpha_{1f}}$, $C_{\alpha_{1r}}$, C_{α_2} and trailer yaw moment of inertia I_{2zz} were estimated simultaneously with DEKF.

In order to improve the performance of the parameter estimation algorithm, the stiffness of the tyres on the tractor front axle was assumed to be known. A value of $C_{\alpha_{1f}} = -4.20 \times 10^5$ N/rad was used for the steering axle in the laden case. This is based on the manufacturer's data for this tyre.

The measurements of system outputs were tractor yaw rate $\dot{\psi}_1$ and trailer yaw rate $\dot{\psi}_2$. The corresponding measurement noise covariance matrix $\mathbf{R}$ was set the same as in Equation (10).

The initial parameter covariance matrix $\mathbf{Q}_p$ was set as follows:

$$\mathbf{Q}_p = \begin{bmatrix} (600)^2 & 0 & 0 \\ 0 & (1000)^2 & 0 \\ 0 & 0 & (400)^2 \end{bmatrix} \begin{bmatrix} C_{\alpha_{1r}} \\ C_{\alpha_2} \\ I_{2zz} \end{bmatrix}, \tag{15}$$

where the square root of the terms of $\mathbf{Q}_p$ are approximately 0.1% of the values of the estimated parameters. The forgetting factor λ was set as 0.9995.

The estimation results from all of the tests were similar. Only one of them is shown. Figure 7 shows the parameter estimation results for the tyre cornering stiffness of trailer axles and trailer yaw moment of inertia. The estimated values of the tyre cornering stiffnesses of tractor drive axle, trailer axles, and trailer yaw moment of inertia are $C_{\alpha_{1r}} = -1.12 \times 10^6$ N/rad, $C_{\alpha_2} = -1.66 \times 10^6$ N/rad, and $I_{2zz} = 3.59 \times 10^5$ kgm^2.

By adding the yaw moment of inertia of unladen trailer and the yaw moment of inertia of the fully filled water tanks around the trailer whole mass CoG, the yaw moment of inertia of fully laden trailer is approximately 3.80×10^5 kgm^2. It can be seen from Figure 7 that the estimated value of the trailer yaw moment of inertia $I_{2zz} = 3.59 \times 10^5$ kgm^2 is approximately 6% below the reference value.

There are several possible reasons for the estimation error, including nonlinearity of the vehicle parameters, offsets of the sensor signals, inaccurate values of the assumed tractor yaw moment of inertia I_{1zz}, and assumed cornering stiffness of the tyres on the tractor front axle $C_{\alpha_{1f}}$.

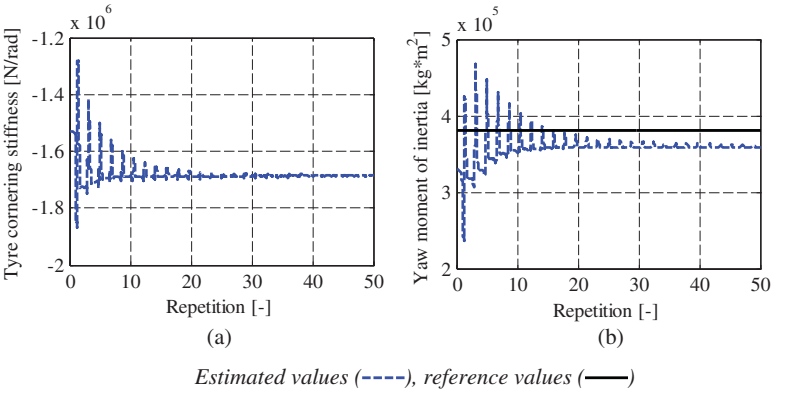

Figure 7. Estimation of $C_{\alpha 2}$ and I_{2zz} for test vehicle: (a) tyre cornering stiffness of all tyres on trailer axles; (b) trailer yaw moment of inertia.

4.3. *Height of trailer sprung mass CoG and trailer roll moment of inertia*

With the estimated values of tyre cornering stiffnesses and yaw moment of inertia of trailer, the height of the payload in the trailer was estimated with the estimation algorithm and the height of trailer sprung mass CoG and trailer roll moment of inertia were calculated.

The height of unladen trailer sprung mass CoG was assumed to be 1.20 m, and the roll moment of inertia of the unladen trailer about its roll axis was $I_{2sx'x'} = 1.27 \times 10^4\,\mathrm{kgm}^2$.

The measurements were tractor roll rate $\dot{\phi}_1$, trailer roll rate $\dot{\phi}_2$, tractor yaw rate $\dot{\psi}_1$, and trailer yaw rate $\dot{\psi}_2$. The corresponding measurement noise covariance matrix $\mathbf{R}$ was set the same as in Equation (12).

The initial parameter covariance matrix $\mathbf{Q}_p$ was set the same as in Equation (13), and the forgetting factor was set as $\lambda = 0.9995$. The initial value of the height of payload above the floor of the trailer was set as 0.1 m. The estimated tyre cornering stiffnesses and trailer yaw moment of inertia, from the vehicle testing data in Section 4.2, were used to estimate the height of the payload.

Figure 8 shows the estimation results for the height of payload from the trailer floor. The estimated value of the height of payload is shown as dashed line. The reference value (the height of the water tanks is 1.145 m) is shown as solid line. The estimated payload height was 1.257 m, which is slightly different from the reference value. This is mostly due to the inaccuracy of the suspension roll stiffness and damping used in the estimation algorithm.

The height of trailer sprung mass CoG and the trailer roll moment of inertia was calculated as $h_{2s} = 1.609$ m and $I_{2sx'x'} = 4.40 \times 10^4\,\mathrm{kgm}^2$.

It can be seen that the two-stage estimation procedure yields good results.

It also can be seen that it takes more than 10 repetitions for the estimated parameters to converge at both stages above, as shown in Figures 7 and 8. Currently, the parameter estimation algorithm can only be used off-line with the measurements in vehicle tests. This convergence time is not an issue for off-line estimation. But it may restrict the online application of the algorithms.

4.4. *Vehicle state estimation*

When all the vehicle parameters were available, the vehicle states were estimated using the state estimator.

The measurements were tractor roll rate $\dot{\phi}_1$, trailer roll rate $\dot{\phi}_2$, tractor yaw rate $\dot{\psi}_1$, and trailer yaw rate $\dot{\psi}_2$. The corresponding measurement noise covariance matrix $\mathbf{R}$ was set the same as in Equation (12), and the process noise covariance $\mathbf{Q}_x$ was set the same as Equation (14).

Figure 9 shows the estimated vehicle states in a lane change manoeuvre with fully laden trailer. It can be seen that the estimated sideslip at the position of the landing leg in both conditions are close to the reference values measured by the optical sensor.

The estimated values generated by the KF have much less noise than the measured signal. This will improve the performance of the active trailer steering controller developed by Jujnovich and Cebon [22].

Overall, the two-step method can estimate the parameters off-line, with good accuracy in comparison with the measurements in vehicle test. There are difficulties with online real-time applications due to the nature of two-step estimation and the convergence time. Further investigation is needed for real-time application of the parameter estimation algorithm.

In addition, road camber, nonlinear tyre characteristics, and varying road surface conditions, which are highly coupled with sideslip and tyre cornering stiffness, are not included in this article. This will limit the practical applications of the estimation algorithms.

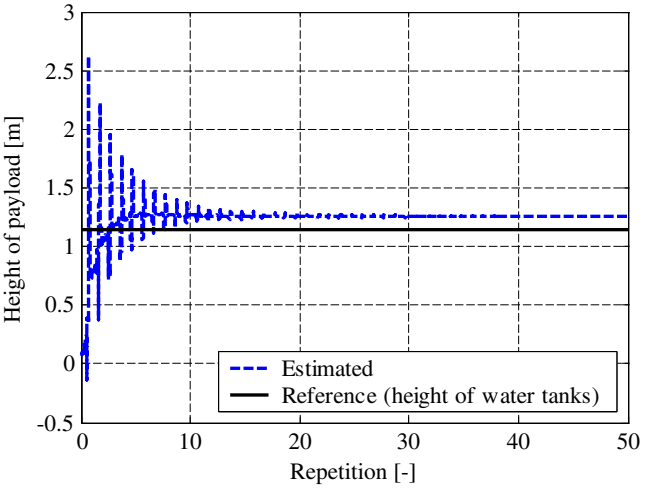

Figure 8. Estimation of h_{2p} for the test vehicle.

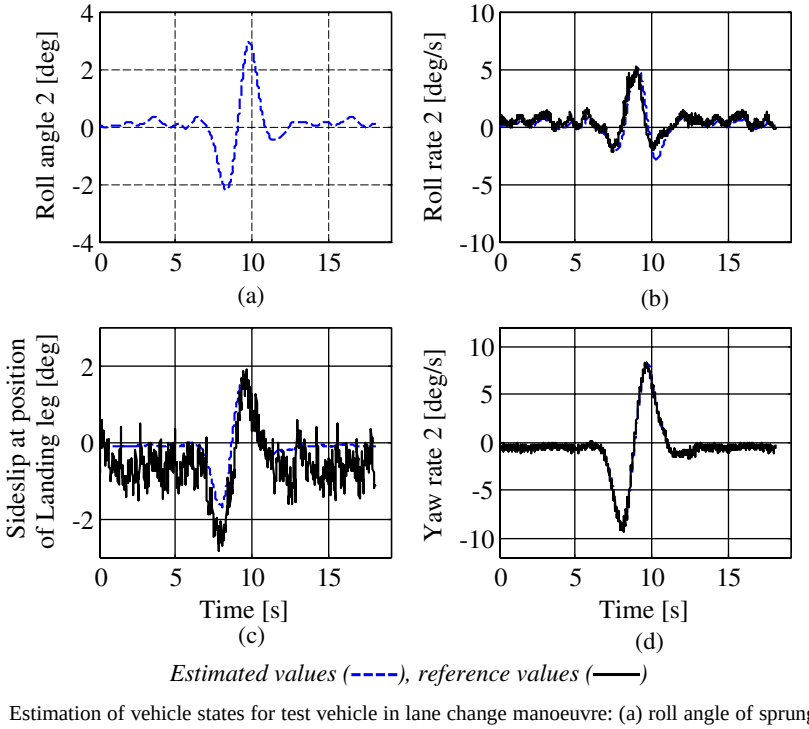

Figure 9. Estimation of vehicle states for test vehicle in lane change manoeuvre: (a) roll angle of sprung mass of trailer; (b) roll rate of sprung mass of trailer; (c) sideslip angle at position of trailer landing leg; and (d) yaw rate of sprung mass of trailer.

5. Conclusions

(1) A model-based KF was designed for vehicle state estimation.
(2) Estimation algorithms based on the DEKF were designed to estimate the vehicle states and parameter values simultaneously.

(3) Simulation results using a nonlinear plant model in TruckSim showed that the linear parameter estimation algorithm could achieve a reasonably accurate estimation of vehicle parameters, considering the nonlinearity of the plant vehicle model and the signal noise. The model-based estimator gave good estimates of vehicle states for low lateral acceleration levels, even though there may be some modest errors in the estimated vehicle parameters.
(4) Experiments were conducted to verify the vehicle parameter and state estimation algorithms. The experimental study verified the viability of the estimation approach for an experimental vehicle.

Acknowledgements

The authors would like to acknowledge the members of the Cambridge Vehicle Dynamics Consortium, who supported the work in this article. At the time of writing the members were: ArvinMeritor, Camcon, Denby Transport, Firestone Industrial Products, Fluid Power Design, FM Engineering, Fruehauf, Goodyear Tyres, Haldex Brake Products, Intec Dynamics, Mektronika Systems, MIRA Limited, Qinetiq, Shell UK Ltd, Tinsley Bridge Ltd, and Volvo Global Trucks. Thanks also to Dr Richard Roebuck, Dr Andrew Odhams, and Mr Jonathan Miller for their assistance with the project.

Nomenclature

Superscripts and subscripts	
$\square_i$	variable of the ith unit of articulated heavy vehicle (ϕ, β, ψ)
For the vehicle of tractor semitrailer, 1-tractor, 2-semitrailer	
$\dot{\square}$	first-time derivative of the variable (ϕ, β, ψ)
$\ddot{\square}$	second-time derivative of the variable (ϕ, ψ)
$\mathbf{A}$, $\mathbf{B}$	matrices of continuous-time state–space representation
$\mathbf{A}_d$, $\mathbf{B}_d$, $\mathbf{C}_d$, $\mathbf{D}_d$	matrices of discrete-time state–space representation
$C_{1f/r}$	roll damping of front/rear suspension of tractor (N/rad)
C_2	roll damping of all suspensions of semitrailer (N/rad)
$C_{\alpha_{1f/r}}$	tyre cornering stiffness of tyres on the front/rear axle of tractor (N/rad)
C_{α_2}	tyre cornering stiffness of all tyres of trailer (N/rad)
D_p	width of payload in trailer (m)
$F_{y_{12c}}$	lateral component of directional forces at coupling point between tractor and semitrailer (N) (pointing in the direction of y-axis on the tractor, pointing in the opposite direction of y-axis on the semitrailer)
$\mathbf{I}$	identity matrix
$I_{2sx'x'_e}$	roll moment of inertia of sprung mass of empty trailer, measured about roll axis of trailer (kgm^2)
I_{isxx}	roll moment of inertia of sprung mass of vehicle unit i, measured about CoG centre of sprung mass (kgm^2)
$I_{isx'x'}$	roll moment of inertia of sprung mass of vehicle unit i, measured about roll axis of vehicle unit i (kgm^2) (=$I_{isxx} + m_{is}\,(h_{is} - h_{ir})^2$)
I_{isxz}	roll/yaw product of inertia of sprung mass of vehicle unit i, measured about CoG centre of sprung mass (kgm^2)
I_{izz}	yaw moment of inertia of whole mass of vehicle unit i, measured about CoG centre of whole vehicle mass (kgm^2)
J	cost function of optimal control
$\mathbf{K}$	vector of gains in the optimal control
$K_{1f/r}$	roll stiffness of front/rear suspension of tractor (Nm/rad)
$K_{1tf/r}$	roll stiffness of front/rear axle and tyres of tractor (Nm/rad)
$K^*_{1f/r}$	roll stiffness of front/rear suspension of tractor adjusted with tyre vertical stiffness (Nm/rad) ($1/K^*_{1f/r} = (1/K_{1f/r}) + (1/K_{1tf/r})$)
K_2	roll stiffness of trailer suspensions (Nm/rad)
K_{2t}	roll stiffness of trailer axles with tyres (Nm/rad)
K^*_2	roll stiffness of trailer suspensions adjusted with tyre verticals stiffness (Nm/rad) ($1/K^*_2 = (1/K_2) + (1/K_{2t})$)
K_{12}	roll stiffness of coupling point between tractor and semitrailer (Nm/rad)
$N(,)$	normal probability distribution
N_{β_i}	$\partial M_z/\partial\beta = \sum_j x_{i,j} C_{\alpha_{ij}}$, partial derivative of net tyre yaw moment w.r.t. sideslip angle (Nm/rad)

$N_{\delta_{1f}}$	$\partial M_z/\partial\delta_{1f} = -x_{1f}C_{\alpha_{1f}}$, partial derivative of net tyre yaw moment of tractor front axle w.r.t. steer angle (Nm/rad)
$N_{\delta_{2f/m/r}}$	$\partial M_z/\partial\delta_{2f/m/r} = -x_{2,f/m/r}C_{\alpha_{2f/m/r}}$, partial derivative of net tyre yaw moment of each trailer axle w.r.t. steer angle (Nm/rad)
$N_{\dot{\psi}_i}$	$\partial M_z/\partial\dot{\psi}_i = \sum_j l_{i,j}^2 C_{\alpha_{ij}}/u$, partial derivative of net tyre yaw moment w.r.t. yaw rate (Nm/(rad/s))
$\mathbf{Q}_p$	parameter covariance matrix
$\mathbf{Q}_x$	process noise covariance matrix
$\mathbf{R}$	measurement noise covariance matrix
T	time step
Y_{β_i}	$\partial F_y/\partial\beta = \sum C_{\alpha_{ij}}$ (jth axle on the vehicle unit i), partial derivative of net tyre lateral force w.r.t. sideslip angle (N/rad)
$Y_{\delta_{1f}}$	$\partial F_y/\partial\delta_{1f} = -C_{\alpha_{1f}}$, partial derivative of net tyre lateral force of tractor front axle w.r.t. steer angle (N/rad)
$Y_{\delta_{2f/m/r}}$	$\partial F_y/\partial\delta_{2f/m/r} = -C_{\alpha_{2f/m/r}}$, partial derivative of net tyre lateral force of each trailer axle w.r.t. steer angle (N/rad)
$Y_{\dot{\psi}_i}$	$\partial F_y/\partial\dot{\psi}_i = \sum_j l_{i,j}C_{\alpha_{ij}}/u_i$, partial derivative of net tyre lateral force w.r.t. yaw rate (N/(rad/s))
g	gravity constant (m/s^2)
h_{2f}	height of trailer floor from the ground (m)
h_{2p}	height of payload from the trailer floor (m)
h_{2s_e}	height of sprung mass CoG of unladen trailer, measured upwards from the ground (m)
h_{ic}	height of coupling point on vehicle unit i, measured upwards from the ground (m)
h_{icr}	height of coupling point on vehicle unit i, measured upwards from roll axis of sprung mass of vehicle unit i (m)
h_{ir}	height of roll centre of sprung mass of vehicle unit i, measured upwards from the ground (m)
h_{is}	height of sprung mass CoG of vehicle unit i, measured upwards from the ground (m)
k	discrete-time instant kT in discrete-time state–space equations
$l_{1f/r}$	distance between the whole mass CoG of tractor and the front/rear axle (m)
l_{2r}	distance between the whole mass CoG of semitrailer and the middle trailer axle (m)
l_{2ce}	distance between the fifth wheel and the trailer rear end (m)
l_{ic}	distance between the whole mass CoG of vehicle unit i and the coupling point (m)
l_{ie}	distance between the whole mass CoG of vehicle unit i and the rear end of the same vehicle unit (m)
m_{2s_e}	sprung mass of empty unladen trailer (kg)
m_i	total mass of vehicle unit i (kg)
m_{is}	sprung mass of vehicle unit i (kg)
$\hat{\mathbf{p}}$	vector of estimated parameters
$\mathbf{u}$	input vector
u_i	longitudinal velocity of vehicle unit i (m/s)
$\mathbf{v}$	output noise vector
$\mathbf{w}$	process noise vector
$\mathbf{x}$	vector of vehicle states
$\hat{\mathbf{x}}$	vector of estimated vehicle states
$\mathbf{y}$	output vector
$\alpha_{if/m/r}$	tyre slip angle of front/middle/rear axle of vehicle unit i (rad)
β_i	sideslip angle of vehicle body of vehicle unit i on roll axis under the whole vehicle mass CoG position (rad)
$\delta_{if/m/r}$	steer angle of tyres on the front/middle/rear axle of vehicle unit i (rad)
λ	forgetting factor in DEKF
ϕ_i	absolute roll angle of sprung mass of vehicle unit i (rad)
ψ_i	yaw angle of vehicle body of vehicle unit i (rad)

References

[1] R. Erhardt, G. Pfaff, and A.T. van Zanten, *Vdc, the vehicle dynamics control system of Bosch*, SAE 950759, 1995, pp. 1419–1436.

[2] A. Hac and M.D. Simpson, *Estimation of vehicle sideslip angle and yaw rate*, SAE Tech. Paper 2000-01-0696, SAE World Congress 2000.

[3] F. Cheli, E. Sabbioni, M. Pesce and S. Melzi, *A methodology for vehicle sideslip angle identification: comparison with experimental data*. Veh. Syst. Dyn. 45(6) (2007), pp. 549–563.

[4] A.Y. Ungoren, H. Peng, and H.E. Tseng, *Experimental verification of lateral speed estimation methods*, Proceedings of the 6th AVEC Conference, Hiroshima, Japan, 2002.

[5] R.E. Kalman, *A new approach to linear filtering and prediction problems.* Trans. ASME, D, J. Basic Eng. 82 (1960), pp. 35–45.

[6] J. Zuurbier and P. Bremmer, *State estimation for integrated vehicle dynamics control*, Proceedings of the 6th AVEC Conference, Hiroshima, Japan, 2002.

[7] A. Hac and M.D. Simpson, *Estimation of vehicle side slip angle and yaw rate*, SAE 2000-01-0696, 2000.
[8] A.Y. Ungoren, H. Peng, and H.E. Tseng, *A study on lateral speed estimation methods.* Int. J. Veh. Auton. Syst. 2(1/2) (2004), pp. 126–144.
[9] W. Sienel, *Estimation of the tire cornering stiffness and its application to active car steering*, Proceedings of the 36th IEEE Conference on Decision and Control, San Diego, CA, 1997.
[10] W. Kober and W. Hirschberg, *On-board payload identification for commercial vehicles*, IEEE International Conference on Mechatronics, Budapest, Hungary, 2006.
[11] T.A. Wenzel, K.J. Burnham, M.V. Blundell, and R.A. Williams, *Dual extended Kalman filter for vehicle state and parameter estimation.* Veh. Syst. Dyn. 44(2) (2006), pp. 153–171.
[12] L. Segel, *Theoretical prediction and experimental substantiation of the response of the automobile to steering control*, Proceedings of IMechE Automobile Division, 1956–1957, London.
[13] R.C. Lin, D. Cebon, and D.J. Cole, *Active roll control of articulated vehicles.* Veh. Syst. Dyn. 26 (1996), pp. 17–43.
[14] D.J.M. Sampson and D. Cebon, *Achievable roll stability of heavy road vehicles.* Proc. Inst. Mech. Eng., J. Automob. Eng. 217(4) (2003), pp. 269–287.
[15] E.A. Wan and A.T. Nelson, *Dual Kalman filtering methods for nonlinear prediction, smoothing, and estimation*, in *Advances in Neural Information Processing Systems*, M.C. Mozer, M.I. Jordan and F. Petsche eds., The MIT Press, MA, USA, 1997.
[16] E.A. Wan and A.T. Nelson, *Dual extended Kalman filter methods*, in *Kalman Filtering and Neural Networks*, Chapter 5, S. Haykin, ed., John Wiley & Sons, New York, 2001.
[17] C. Cheng, *Enhancing safety of actively-steered articulated vehicles*, Ph.D. diss., University of Cambridge, Cambridge, UK, 2009.
[18] E.A. Wan and A.T. Nelson, *Removal of noise from speech using the dual Ekf algorithm*, Proceedings of the International Conference on Acoustics, Speech, and Signal Processing, ICASSP'98, Seattle, USA, 1998.
[19] Society of Automotive Engineers, *A test for evaluating the rearward amplification of multi-articulated vehicles*, SAE Recommended Practice J2179, Warrendale, USA, 1993.
[20] A.J.P. Miege and D. Cebon, *Active roll control of an experimental articulated vehicle.* Proc. Inst. Mech. Eng., J. Automob. Eng. 219(6) (2005), pp. 791–806.
[21] R.L. Roebuck, et al., *A systems approach to controlled heavy vehicle suspension.* Int. J. Heavy Veh. Syst. 12(3) (2005), pp. 169–192.
[22] B.A. Jujnovich and D. Cebon, *Path-following steering control for articulated vehicles.* ASME J. Dyn. Syst. Meas. Control (2010), in press.
[23] B.P. Jeppesen and D. Cebon, *Application of observer-based fault detection in vehicle roll control.* Veh. Syst. Dyn. 47(4) (2009), pp. 465–495.
[24] Correvit S-400, *Non-contact optical sensor user manual*, Corrsys-Datron Sensorsysteme GmbH, Wetzlar, Germany, 2006.

Appendix

The equations representing the motion of the tractor are (refer to the list of Nomenclature and Figure 1 for definitions of the symbols) as follows:

$$m_1u_1(\dot{\beta}_1+\dot{\psi}_1)-m_{1s}(h_{1s}-h_{1r})\ddot{\phi}_1=Y_{\beta_1}\beta_1+Y_{\dot{\psi}_1}\dot{\psi}_1+Y_{\delta_{1f}}\delta_{1f}+F_{y_{12c}}, \tag{A1}$$

$$-I_{1sxz}\ddot{\phi}_1+I_{1zz}\ddot{\psi}_1=N_{\beta_1}\beta_1+N_{\dot{\psi}_1}\dot{\psi}_1+N_{\delta_{1f}}\delta_{1f}-F_{y_{12c}}l_{1c}, \tag{A2}$$

$$\begin{aligned}[I_{1sxx}+m_{1s}(h_{1s}-h_{1r})^2]\ddot{\phi}_1-I_{1sxz}\ddot{\psi}_1=m_{1s}g(h_{1s}-h_{1r})\phi_1+m_{1s}(h_{1s}-h_{1r})[u_1(\dot{\beta}_1+\dot{\psi}_1)-(h_{1s}-h_{1r})\ddot{\phi}_1]\\ -(K^*_{1f}+K^*_{1r})\phi_1-(C_{1f}+C_{1r})\dot{\phi}_1+K_{12}(\phi_2-\phi_1)-F_{y_{12c}}h_{1cr}.\end{aligned} \tag{A3}$$

Since the roll motion of axles is neglected in the equations, the resultant roll stiffness K^*_{1f} and K^*_{1r} caused by both suspension and tyre are calculated by $1/K^*_{1f}=(1/K_{1f})+(1/K_{1tf})$ and $1/K^*_{1r}=(1/K_{1r})+(1/K_{1tr})$.

The equations representing the motion of semitrailer are as follows:

$$m_2u_2(\dot{\beta}_2+\dot{\psi}_2)-m_{2s}(h_{2s}-h_{2r})\ddot{\phi}_2=Y_{\beta_2}\beta_2+Y_{\dot{\psi}_2}\dot{\psi}_2+Y_{\delta_{2f}}\delta_{2f}+Y_{\delta_{2m}}\delta_{2m}+Y_{\delta_{2r}}\delta_{2r}-F_{y_{12c}}, \tag{A4}$$

$$-I_{2sxz}\ddot{\phi}_2+I_{2zz}\ddot{\psi}_2=N_{\beta_2}\beta_2+N_{\dot{\psi}_2}\dot{\psi}_2+N_{\delta_{2f}}\delta_{2f}+N_{\delta_{2m}}\delta_{2m}+N_{\delta_{2r}}\delta_{2r}-F_{y_{12c}}l_{2c}, \tag{A5}$$

$$\begin{aligned}[I_{2sxx}+m_{2s}(h_{2s}-h_{2r})^2]\ddot{\phi}_2-I_{2sxz}\ddot{\psi}_2=m_{2s}g(h_{2s}-h_{2r})\phi_2+m_{2s}(h_{2s}-h_{2r})[u_2(\dot{\beta}_2+\dot{\psi}_2)-(h_{2s}-h_{2r})\ddot{\phi}_2]\\ -K^*_2\phi_2-C_2\dot{\phi}_2-K_{12}(\phi_2-\phi_1)+F_{y_{12c}}h_{2cr}.\end{aligned} \tag{A6}$$

Similarly, the resultant roll stiffness K_2^* due to tyre and suspension stiffness are calculated by

$$\frac{1}{K_2^*} = \frac{1}{K_2} + \frac{1}{K_{2t}}.$$

The kinematic constraint equation between the tractor and the semitrailer is given by

$$\dot{\beta}_2 = \dot{\beta}_1 - \frac{h_{1c} - h_{1r}}{u_1}\ddot{\phi}_1 + \frac{h_{2c} - h_{2r}}{u_2}\ddot{\phi}_2 - \frac{l_{1c}}{u_1}\ddot{\psi}_1 - \frac{l_{2c}}{u_2}\ddot{\psi}_2 + \dot{\psi}_1 - \dot{\psi}_2. \tag{A7}$$